Receptor-Mediated DNA-Targeted Photoimmunotherapy

Tom C. Karagiannis,[1,2] Pavel N. Lobachevsky,[1] Brenda K.Y. Leung,[3] Jonathan M. White,[3] and Roger F. Martin[1,3]

[1]Molecular Radiation Laboratory, Research Division, Peter MacCallum Cancer Centre, East Melbourne, Victoria, Australia and [2]Department of Pathology and [3]School of Chemistry, The University of Melbourne, Parkville, Victoria, Australia

Abstract

We show the efficacy of a therapeutic strategy that combines the potency of a DNA-binding photosensitizer, UV_A*Sens*, with the tumor-targeting potential of receptor-mediated endocytosis. The photosensitizer is an iodinated bibenzimidazole, which, when bound in the minor groove of DNA and excited by UV_A irradiation, induces cytotoxic lesions attributed to a radical species resulting from photodehalogenation. Although reminiscent of photochemotherapy using psoralens and UV_A irradiation, an established treatment modality in dermatology particularly for the treatment of psoriasis and cutaneous T-cell lymphoma, a critical difference is the extreme photopotency of the iodinated bibenzimidazole, ~1,000-fold that of psoralens. This feature prompted consideration of combination with the specificity of receptor-mediated targeting. Using two *in vitro* model systems, we show the UV_A cytotoxicity of iodo ligand/protein conjugates, implying binding of the conjugate to cell receptors, internalization, and degradation of the conjugate-receptor complex, with release and translocation of the ligand to nuclear DNA. For ligand-transferrin conjugates, phototoxicity was inhibited by coincubation with excess native transferrin. Receptor-mediated UV_A-induced cytotoxicity was also shown with the iodo ligand conjugate of an anti-human epidermal growth factor receptor monoclonal antibody, exemplifying the potential application of the strategy to other cancer-specific targets to thus improve the specificity of phototherapy of superficial lesions and for extracorporeal treatments. (Cancer Res 2006; 66(21): 10548-52)

Introduction

The accumulation of examples of targeted cancer therapy indicates that the long-heralded potential of antitumor antibodies is finally being realized (1, 2). Although in some cases the biological activity of the antibody itself can be useful, as for Herceptin (3) usually the tumor-targeting feature needs to be combined with some sort of cytotoxic mechanism. The classic example is the use of radioactively labeled antibodies in radioimmunotherapy, which is now an established treatment for lymphoma (1). In developing nonradioactive cytotoxic moieties for conjugation with antibodies, the finite number of receptors associated with tumor-targeting systems imposes demanding requirements on cytotoxic potency. After earlier exploration of potent bacterial toxins, the most promising response to this challenge seems to be Mylotarg, which exploits the cytotoxic potency of enediynes, in immunoconjugates of an anti-CD33 monoclonal antibody with calicheamicin (4).

Unfortunately, the specificity of antitumor antibodies is not absolute, and although continuing improvements can be expected, there is an obvious attraction to strategies that augment tumor targeting. For example, with the use of photosensitizers as the cytotoxic moiety conjugated to tumor-targeting antibodies (5–7), the ability to direct the light beam to the tumor provides an extra dimension to tumor targeting; conjugate taken up by normal tissues outside the illuminated area is not activated. However, the photopotency of most photosensitizers relative to the numbers of molecules that can be delivered by receptor-mediated endocytosis seems likely to impose limitations. Accordingly, the photopotency of the iodinated minor groove-binding bibenzimidazole, as well as being of interest per se, is important in the context of targeted therapy.

The development of iodinated DNA minor groove-binding bibenzimidazoles as UV_A sensitizers (8) was prompted by the classic studies with DNA-incorporated halogenated DNA precursors, photoactivation of which results in dissociation of the carbon-halogen bond forming a uracilyl free radical, inducing DNA strand breakage by abstraction of H atoms from deoxyribosyl carbons (9). Previously, we investigated several iodinated bibenzimidazoles, which induce DNA damage and cytotoxic lesions due to radical species formed by UV_A-mediated photodehalogenation (8, 10). The DNA-binding ligand now denoted UV_A*Sens* (Fig. 1*A, 2*) proved to be outstanding with respect to photopotency compared with the other isomers due in part to the very high quantum yield of photodeiodination (11, 12). When using 1 μm UV_A*Sens*, the UV_A fluence required for 90% cell kill is ~2 J/m^2 (11), whereas for UV_A/psoralens [an established therapy for psoriasis (13) and cutaneous T-cell lymphoma (14)] or visible light/porphyrin photosensitizers [approved for therapy of certain cancers (15) and macular degeneration (16)], the fluences required for comparable cell kill are ~3 orders of magnitude higher (17–20). Given the extreme photopotency of UV_A*Sens*, we developed conjugates to direct the drug to specific target cells via receptor-mediated endocytosis, and we establish proof of principle *in vitro* using two model systems involving transferrin and epidermal growth factor receptor (EGFR) internalization.

Materials and Methods

Cells, transferrin, antibodies, incubations, and UV irradiation. Human chronic myelogenous leukemia K562 cells, which express ~1.5 × 10^5 transferrin receptors per cell, were grown in suspension in RPMI 1640 supplemented with 20 mmol/L HEPES (pH 7.4), 10% (v/v) fetal bovine serum (FBS; Commonwealth Serum Laboratories, Parkville, Victoria, Australia), 2 mmol/L L-glutamine, and 80 μg/mL gentamicin. Human epidermoid carcinoma A431 cells, which express ~2 × 10^6 EGFRs per cell, and Chinese hamster ovary CHO-K1 cells were grown in α modified Eagle's

Note: Supplementary data for this article are available at Cancer Research Online (http://cancerres.aacrjournals.org).

Requests for reprints: Roger F. Martin, Peter MacCallum Cancer Centre, Research Level 2, Locked Bag No. 1, A'Beckett Street, East Melbourne, Victoria, Australia. E-mail: roger.martin@petermac.org.

©2006 American Association for Cancer Research.

doi:10.1158/0008-5472.CAN-06-1853

Downloaded from cancerres.aacrjournals.org on April 13, 2017. © 2006 American Association for Cancer Research.

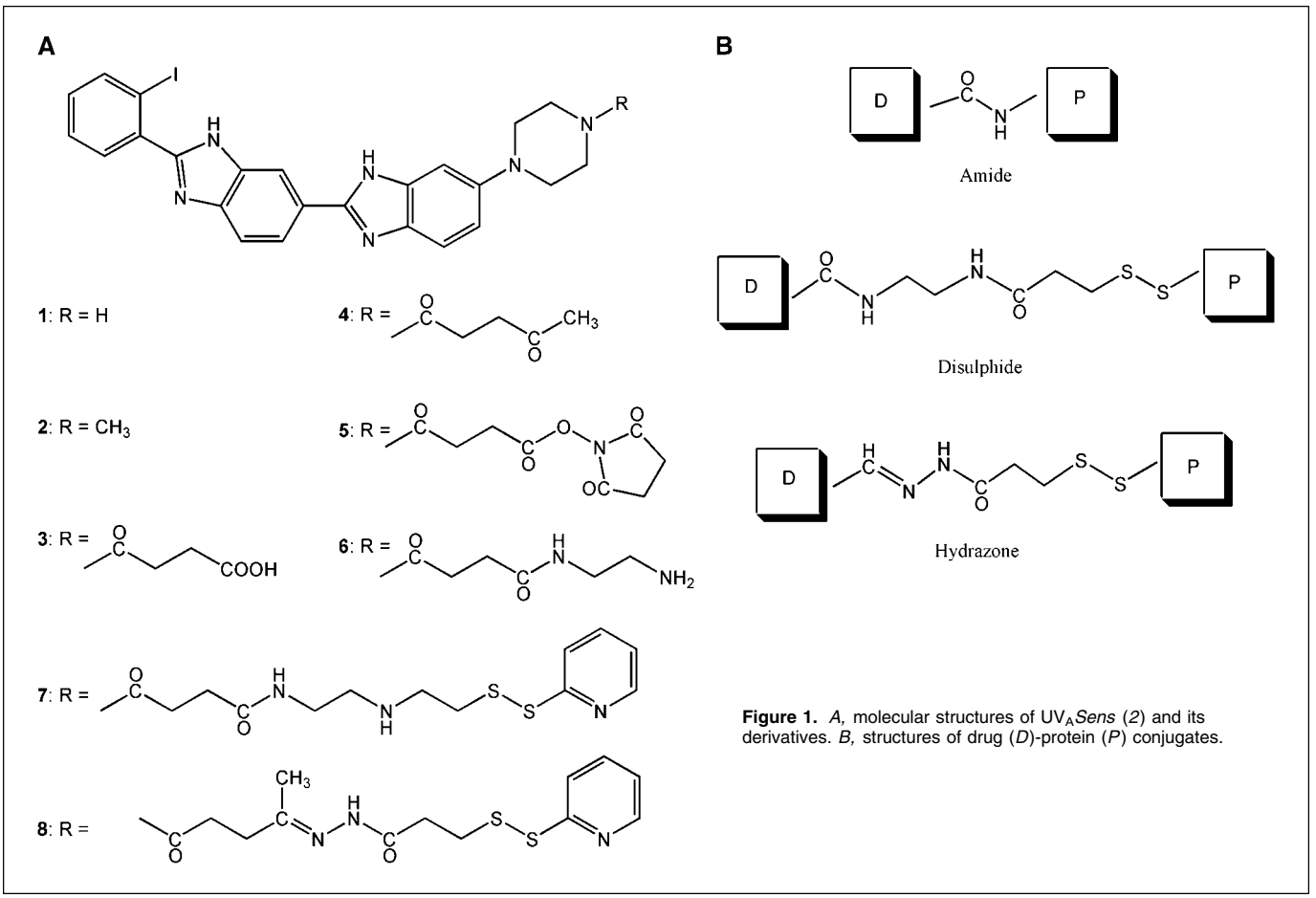

Figure 1. *A,* molecular structures of UV_A*Sens* (*2*) and its derivatives. *B,* structures of drug (*D*)-protein (*P*) conjugates.

medium supplemented with 20 mmol/L HEPES (pH 7.4), 10% (v/v) FBS, 2 mmol/L L-glutamine, and 80 μg/mL gentamicin.

Human serum apo-transferrin was purchased from the Sigma Chemical Co. Ltd. (St. Louis, MO). To optimize the binding of transferrin to cell surface transferrin receptors on K562 cells, human serum apo-transferrin was fully saturated with iron to yield diferric transferrin as described previously (21).

The hybridoma producing the murine A225 (IgG1) monoclonal antibody (MoAB-225), which binds to human EGFRs, was obtained from the American Type Culture Collection (Manassas, VA; HB-8508). Antibody was purified from cell culture supernatants using HiTrap protein G affinity columns according to the manufacturer's protocols (Amersham Biosciences, Piscataway, NJ).

Transferrin and MoAB-225 was thiolated by adding the heterobifunctional cross-linking reagent succinimidyl 3-(-2-pyridyldithio)-propionate (SPDP) as detailed in the Supplementary Data (Pierce Chemical Co., Rockford, IL) in absolute ethanol to protein in 100 mmol/L sodium phosphate buffer (pH 7.5) to give a 10-fold molar excess of SPDP to protein. The reaction mixture was incubated for 1 hour at room temperature. Excess unreacted SPDP was removed by gel filtration chromatography using a NAP-5 column (Sephadex G-25, Phamacia Biotech, Inc., Piscataway, NJ) that had been equilibrated with 100 mmol/L sodium acetate buffer (pH 4.5). The dithiopyridyl protecting groups were then removed by reduction of the disulfide bond by reaction with a 10-fold molar excess of DTT for 30 minutes at room temperature. Thiolated proteins were purified immediately by gel filtration chromatography using a NAP-5 or NAP-10 column (Sephadex G-25) that had been equilibrated with 100 mmol/L sodium phosphate buffer (pH 7.5).

Washed K562 cells were incubated with UV_A*Sens*-transferrin conjugates (final protein concentration, 200 nmol/L) in the presence and absence of a 50-fold molar excess of diferric transferrin in serum-free RPMI 1640 for 20 hours at 37°C, washed twice, and then irradiated with a series of UV_A fluences (15 W NEC black light fluorescent lamps; emission maximum at 360 nm, flux of 0.25-0.50 W/m^2). After UV_A irradiation, K562 cells were isolated by centrifugation at 400 × *g* for 3 minutes and cloned in semisolid (0.33%, w/v) noble agar in triplicate in six-well microtiter plates as described previously (22). Colonies containing at least 50 cells were counted 14 days after cloning. The control plating efficiency of untreated K562 cells was in the range of 40% to 50%. Assay of clonogenic survival of A431 and CHO-K1 cells is described in the Supplementary Data (Supplementary Fig. S2). The results (mean ± SD of triplicate plating) from a single representative experiment are shown. At least three independent experiments were done for all cell lines, and each of the conjugates and the results between experiments were consistent, typically differing by less than ±10%.

Preparation of conjugates. The bibenzimidazole precursors for the protein- UV_A*Sens* conjugates were synthesized by methods described in detail previously (23), except using piperazine instead of *N*-methylpiperazine, thus yielding 1 rather than 2. The carboxylic acid (Fig. 1*A, 3*) and carbonyl (Fig. 1*A, 4*) analogues were prepared by reacting 1 with succinic acid anhydride or the anhydride levulinic acid, respectively. The purified compounds were characterized by proton ^1H and carbon ^{13}C nuclear magnetic resonance and by electrospray mass spectrometry. High-performance liquid chromatography, monitored for UV absorbance at 340 nm and for fluorescence (Waters Millipore 420-AC fluorescence detector, Waters Millipore, Billerica, MA), confirmed >95% purity.

Conjugation of UV_A*Sens* to transferrin and MoAB-225 via an amide bond involved direct linkage to aliphatic amine groups (α-amino group of the NH_2-terminal amino acids and the ε-amino group of lysine residues) on the proteins, by reaction with the *N*-hydroxysuccinimidyl ester of the ligand (Fig. 1*A, 5*), which exhibits higher selectivity toward aliphatic amines rather than aromatic amines, alcohols, phenols, such as tyrosine, and histidine.

Downloaded from cancerres.aacrjournals.org on April 13, 2017. © 2006 American Association for Cancer Research.

Thus, reaction of 5 with aliphatic amines in transferrin and MoAB-225 yielded the amide-linked conjugates (Fig. 1*B*).

Preparation of the disulfide- and hydrazone-linked conjugates involved reaction of modified ligand species with thiolated proteins, prepared by reacting primary amine moieties of the protein with the heterobifunctional cross-linking reagent SPDP and then reducing the disulfide bond with excess DTT. For preparation of the disulfide-linked conjugates, the activated ester 5 was reacted with ethylene diamine to produce the ligand amino species (Fig. 1*A, 6*), which was reacted with SPDP to yield the SPDP derivatized ligand (Fig. 1*A, 7*). Reaction of 6 with the free protein thiol groups yields the disulfide-linked conjugates (Fig. 1*B*).

The hydrazone-linked conjugates were prepared by reaction of 4 with the heterobifunctional cross-linking reagent 3-(-2-pyridyldithio)-propionyl hydrazide, and the product was then reacted with the free protein thiol groups, yielding the hydrazone-linked conjugates (Fig. 1*B*).

The conjugates were purified by gel filtration chromatography, and the conjugation numbers (number of iodoHoechst molecules conjugated per protein molecule) were calculated using absorbance spectrophotometry. The conjugates used had conjugation numbers in the range of 1 to 2.5.

Further details are provided in the Supplementary Data (Supplementary Methods).

Results and Discussion

Two experimental systems were used to establish *in vitro* proof of principle of delivery of the halogenated ligand specifically to the DNA of target cells via receptor-mediated endocytosis, involving human erythroleukemic K562 cells and human epidermoid carcinoma A431 cells, which overexpress transferrin and EGFRs, respectively. Although transferrin receptors are expressed on a variety of normal tissues, including maturing erythroid cells, the basal layer of the skin, crypts of the intestinal villi, as well as in the vascular endothelium of brain capillaries, it has been found that the number of transferrin receptors increases several hundred-fold in various tumor cell lines and cancerous tissues (24). Therefore, the transferrin receptor has been considered as a possible cancer cell target (25). However, we chose transferrin receptor–mediated endocytosis in K562 cells as a model experimental system largely because it is so well characterized [$\sim$150,000 per cell (26)] and the ligand (human transferrin) is readily available.

The cell surface transferrin receptor binds the major serum iron transport protein, transferrin, and mediates iron uptake into cells by two distinct pathways. The monensin-resistant pathway via the early acidic (pH $\sim$5) endosomal compartment (27) accounts for approximately 85% to 95% of the internalized transferrin receptors and involves recycling of the apo-transferrin-transferrin receptor complex to the cell surface after release of iron in the endosome. The alternative monensin-sensitive pathway involves transport of approximately 5% to 15% of the cell surface transferrin receptors through the *trans*-Golgi to the lysosomes, leading to degradation of transferrin and transferrin receptors (28).

To show that the targeting system can be easily translated to monoclonal antibodies, we investigated targeting to EGFR, which is overexpressed in a wide range of malignancies, including cancer of the bladder, prostate, lung, pancreas, breast, head and neck, and ovaries (29). Numerous antibodies and small-molecule drugs, such as gefitinib (Iressa, AstraZeneca Corp., Wilmington, DE), targeting EGFRs are currently approved for the treatment of advanced carcinomas or are in clinical trials (30). We used the murine monoclonal antibody A225 and the A431 cell line, which overexpresses the EGFR [$\sim$2 million receptors per cell (31)], as a model system.

We developed three different conjugation chemistries to link the phototoxic UV_A*Sens* analogue to proteins so as to enable intracellular cleavage under different conditions. The key linkage moieties were an amide, cleavable by proteolytic enzymes, a disulfide, cleavable in reducing conditions, and a hydrazone, cleavable in acidic conditions. This approach required modification of UV_A*Sens* to incorporate a carboxylic acid functional group (Fig. 1*A, 3*) for preparation of the amide- and disulfide-linked conjugates or a carbonyl functional group (Fig. 1*A, 4*) for preparation of the hydrazone-linked conjugates (described in Materials and Methods and in Supplementary Methods; Fig. 1*B*). Given the importance of retention of receptor-binding activity, all conjugates were assessed in competition binding assays using ^{125}I-labeled native ligands. The results (Supplementary Table S1) showed that attachment of the iodinated bibenzimidazole moiety to either of the protein ligands does not significantly compromise receptor binding.

Given the innate fluorescence of bibenzimidazole ligands, which is enhanced on binding to DNA, we used quantitative fluorescence microscopy for initial evaluation of the receptor-mediated delivery of the UV_A*Sens* moiety following incubation of the cells with the conjugates. A significant increase in nuclear-associated fluorescence intensity following incubation with the hydrazone-linked conjugate compared with autofluorescence levels of K562 cells was found (Supplementary Fig. S1). The increase in nuclear fluorescence is inhibited by $\sim$3-fold when the cells are incubated with the conjugate in the presence of 100-fold molar excess of unmodified transferrin (Supplementary Fig. S1), confirming that a substantial portion of the fluorescent ligand detected in cell nuclei was delivered by transferrin receptor–mediated processes. However, for cells incubated with disulfide or amide conjugates, the nuclear-associated fluorescence intensity was not significantly different to that observed in untreated K562 cells. Clearly, the acid lability of the hydrazone conjugates was advantageous, consistent with the characteristics of the major transferrin receptor endocytosis pathway.

The results from clonogenic survival assays indicate an UV_A fluence-dependent increase in cytotoxicity of K562 cells following incubation with the conjugates and subsequent UV_A irradiation (Fig. 2). The acid-labile hydrazone-linked conjugate is more efficient than the disulfide-linked conjugate, and the amide-linked conjugate was the least efficient at mediating UV_A-induced phototoxicity. The results also show that the cytotoxicity associated with the disulfide and hydrazone conjugates was largely inhibited by incubation in the presence of 50-fold molar excess unmodified transferrin, indicating that cell death is mediated by transferrin receptors (Fig. 2).

For the EGFR experimental model, we used CHO-K1 cells, which do not express human EGFR, as a control to show that the UV_A phototoxicity was mediated by EGFRs rather than incubating with conjugates in the presence of a large excess of unmodified antibody because MoAB-225 is intrinsically cytotoxic to A431 cells. Investigation of the sensitivity of A431 and CHO-K1 cells to unconjugated UV_A*Sens* and UV_A irradiation indicated that the sensitivity of the two cell lines was similar (Supplementary Fig. S2). Incubation of A431 cells with MoAB-225 conjugates and subsequent UV_A irradiation showed that the UV_A fluence-dependent decrease in survival of A431 cells was similar for all three conjugates (Fig. 3), in contrast to the results obtained using the transferrin model system. This is consistent with the characteristics of the EGFR internalization pathway, which involves trafficking to lysosomes for degradation (32). Importantly, the results also show that the conjugates did not mediate UV_A-induced cytotoxicity in CHO-K1 cells, which do not express human EGFR (Fig. 3).

Downloaded from cancerres.aacrjournals.org on April 13, 2017. © 2006 American Association for Cancer Research.

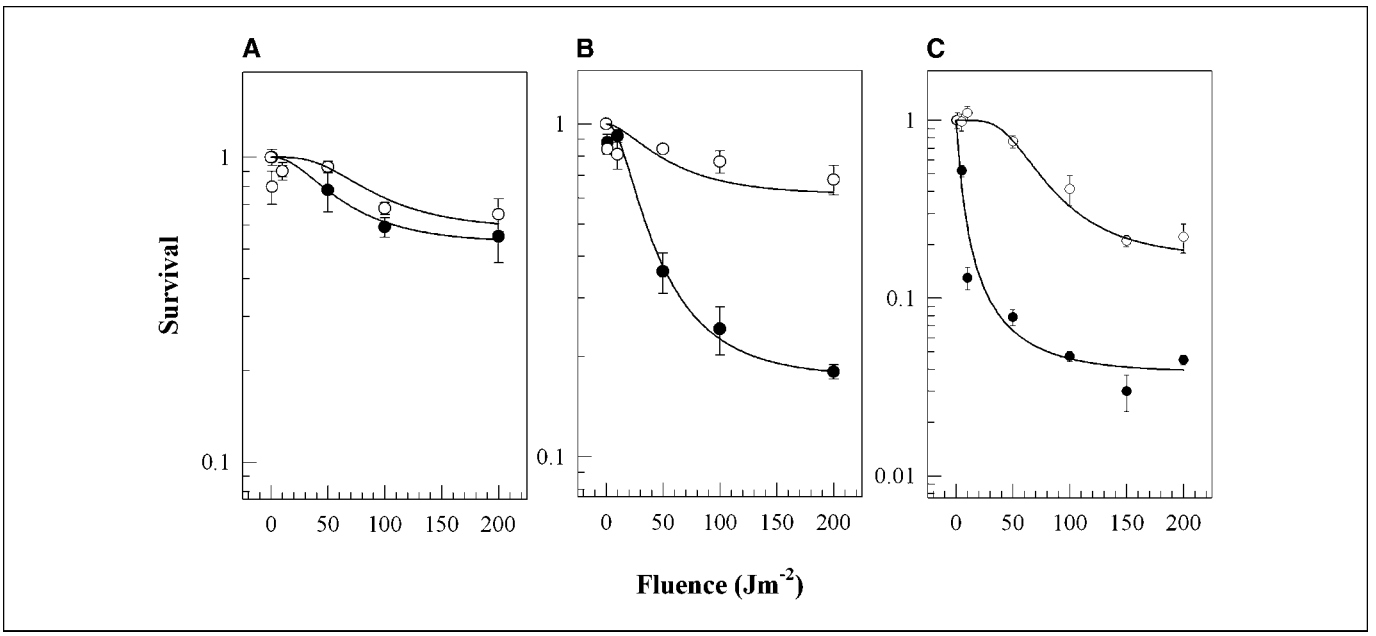

Figure 2. Clonogenic survival of K562 cells following incubation with UV_A*Sens*-transferrin conjugates and UV_A irradiation. Cells were incubated with amide (*A*), disulfide (*B*), and hydrazone (*C*) conjugates (●) at 37°C for 20 hours before UV_A irradiation. ○, in parallel assays, the cells were incubated with the conjugates in the presence of 50-fold molar excess unlabeled transferrin. Conjugation numbers 1.6, 2.5, and 1.5 for the amide, disulfide, and hydrazone conjugates, respectively.

Our earlier studies with K562 cells established empirical relationships between nuclear uptake of unconjugated UV_A*Sens*, UV_A fluence, and cell survival (11), and application of this type of analysis to the survival data from the present studies with the conjugates allows estimation of the extent of nuclear uptake of UV_A*Sens* (Supplementary Table S2). The results confirm that, for the transferrin system, the hydrazone-linked conjugate is degraded more efficiently than the disulfide and amide conjugates. Moreover, the nuclear localization of UV_A*Sens* following incubation with the hydrazone and disulfide/transferrin conjugates is inhibited 10- and 2-fold, respectively, showing the specificity of targeting. These findings are consistent with those from the fluorescence microscopy assays, in which nuclear fluorescence was observed only for the hydrazone conjugate. By contrast, the nuclear uptake of UV_A*Sens* is similar for all three MoAB-225 conjugates, again consistent with the nature of EGFR endocytosis, which involves intralysosomal degradation of the receptor.

An interesting feature of the survival curves (Figs. 2 and 3) is that there is little decrease in survival at UV_A fluences larger than ~ 100 J/m^2. We believe that two factors determine this shape of the

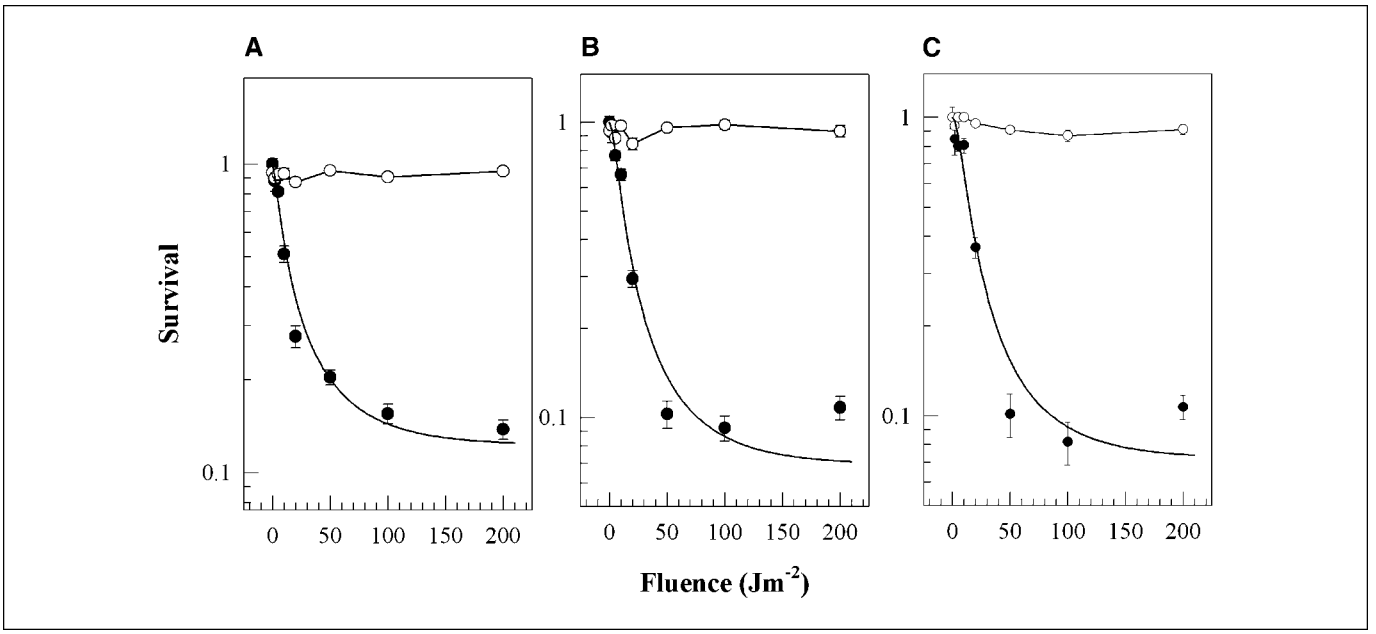

Figure 3. Clonogenic survival of A431 (●) and CHO-K1 (○) cells following incubation with amide (*A*), disulfide (*B*), and hydrazone (*C*) UV_A*Sens*-MoAB-225 conjugates and UV_A irradiation. Conjugation numbers, 1.9, 1.7, and 1.1 for the amide, disulfide, and hydrazone conjugates, respectively.

Downloaded from cancerres.aacrjournals.org on April 13, 2017. © 2006 American Association for Cancer Research.

survival curves. Firstly, one should take into account that the number of cytotoxic lesions in cells is not proportional to the UV_A fluence. Because these lesions result from dehalogenation of the drug, this number saturates as soon as all drug molecules are dehalogenated. We have shown in our previous study with unconjugated photosensitizers (11) that the level at which the survival curve reaches plateau decreases with increasing drug uptake. Therefore, the range of the cell kill achieved with the use of the conjugates reflects the level of the nuclear drug uptake, which is less than can be achieved with the use of unconjugated drug. Secondly, in contrast, for example, to the survival after ionizing radiation for which an exponential model can be applied reflecting the Poisson distribution of stochastic cytotoxic events, for the UV_A/photosensitizer system the numbers of lesions are so large that no significant stochastic variations between cells are expected. Therefore, application of the exponential model fails in this case and we believe that variations between cells in biological variables, such as drug uptake and response to a certain number of cytotoxic lesions, determine the shape of the survival curve. Because the range of these variations is not known, we applied an empirical model to fit the survival curves, which is described in our previous study (11) and in notes to Supplementary Table S2. Parenthetically, in projection of our *in vitro* results to therapeutic scenarios, the extent of cell kill observed (about one log) could prove to be a limitation. However, this feature is likely to be target dependent. Furthermore, it is known that with phototherapy the effect of initial cell kill is amplified by a poorly understood immunomodulatory (33) mechanism and it will be interesting to determine the extent to which UV_A/UV_A*Sens* contributes to this phenomenon in appropriate *in vivo* studies. Additionally, biological variations will be investigated in future studies, particularly exploring other targets.

As for all forms of UV phototherapy, the potential mutagenic activity is a concern, but the targeting feature may ameliorate that concern. Nevertheless, it is important to establish the mutagenic activity of UV_A/UV_A*Sens* treatment, and experiments are planned to address this aspect, for subsequent publications.

In conclusion, we developed a novel strategy for UV_A photoimmunotherapy, combining two levels of targeting, and established proof of principle *in vitro*. As well as directing a potent photosensitizer to DNA, the specificity of receptor-mediated endocytosis is used to target the DNA-binding photosensitizer to tumor cells. In principle, the strategy could be considered as a platform technology potentially adaptable to any cancer-specific cell surface receptor that is internalized, although efficacy will vary depending on the specific pathways of internalization and intracellular degradation. Although the limited penetration of UV_A will confine applicability to superficial lesions and *ex vivo* purging, the use of multiphotonic sources would extend the efficacy range.

Acknowledgments

Received 5/22/2006; revised 7/26/2006; accepted 8/9/2006.

Grant support: National Health and Medical Research Council (NHMRC) grant 209125. The development of the iodinated DNA ligands was supported by earlier grants from NHMRC and the Australian Research Council.

The costs of publication of this article were defrayed in part by the payment of page charges. This article must therefore be hereby marked *advertisement* in accordance with 18 U.S.C. Section 1734 solely to indicate this fact.

References

1. Wu AM, Senter PD. Arming antibodies: prospects and challenges for immunoconjugates. Nat Biotechnol 2005; 23:1137–46.
2. Harris M. Monoclonal antibodies as therapeutic agents for cancer. Lancet Oncol 2004;5:292–302.
3. Toi M, Horiguchi K, Bando H, Saji S, Chow LW. Trastuzumab: updates and future issues. Cancer Chemother Pharmacol 2005;56 Suppl 7:94–9.
4. Fenton C, Perry CM. Gemtuzumab ozogamicin: a review of its use in acute myeloid leukaemia. Drugs 2005;65:2405–27.
5. van Dongen GA, Visser GW, Vrouenraets MB. Photosensitizer-antibody conjugates for detection and therapy of cancer. Adv Drug Deliv Rev 2004;56:31–52.
6. Savellano MD, Pogue BW, Hoopes PJ, Vitetta ES, Paulsen KD. Multiepitope HER2 targeting enhances photoimmunotherapy of HER2-overexpressing cancer cells with pyropheophorbide-a immunoconjugates. Cancer Res 2005;65:6371–9.
7. Hudson R, Carcenac M, Smith K, et al. The development and characterisation of porphyrin isothiocyanate-monoclonal antibody conjugates for photoimmunotherapy. Br J Cancer 2005;92:1442–9.
8. Martin RF, Murray V, D'Cunha G, et al. Radiation sensitization by an iodine-labelled DNA ligand. Int J Radiat Biol 1990;57:939–46.
9. Hutchinson F, Kohnlein W. The photochemistry of 5-bromouracil and 5-iodouracil in DNA. Prog Mol Subcell Biol 1980;7:1–42.
10. Martin RF, Kelly DP, Roberts M, et al. Comparative studies of UV-induced DNA cleavage by structural isomers of an iodinated DNA ligand. Int J Radiat Oncol Biol Phys 1994;29:549–53.
11. Karagiannis TC, Lobachevsky PN, Martin RF. DNA targeted UVA photosensitization: characterization of an extremely photopotent iodinated minor groove binding DNA ligand. J Photochem Photobiol B 2006; 83:195–204.
12. Martin RF, Kelly DP, Roberts M, et al. Comparative studies of UV-induced DNA cleavage by analogues of iodoHoechst 33258. Int J Radiat Biol 1994;66:517–21.
13. Parrish JA, Fitzpatrick TB, Tanenbaum L, Pathak MA. Photochemotherapy of psoriasis with oral methoxsalen and longwave ultraviolet light. N Engl J Med 1974;291: 1207–11.
14. Heald P, Rook A, Perez M, et al. Treatment of erythrodermic cutaneous T-cell lymphoma with extracorporeal photochemotherapy. J Am Acad Dermatol 1992;27:427–33.
15. McCaughan JS, Jr. Photodynamic therapy: a review. Drugs Aging 1999;15:49–68.
16. Michels S, Schmidt-Erfurth U. Photodynamic therapy with verteporfin: a new treatment in ophthalmology. Semin Ophthalmol 2001;16:201–6.
17. Procaccini EM, Selleri C, Monfrecola G, et al. *In vitro* photoinhibition by psoralen and ultraviolet A radiation of human hematopoietic progenitors. Photodermatol Photoimmunol Photomed 1996;12:200–3.
18. Riesenberg R, Fuchs C, Kriegmair M. Photodynamic effects of 5-aminolevulinic acid-induced porphyrin on human bladder carcinoma cells *in vitro*. Eur J Cancer 1996;32A:328–34.
19. Boehncke WH, Konig K, Ruck A, Kaufmann R, Sterry W. *In vitro* and *in vivo* effects of photodynamic therapy in cutaneous T cell lymphoma. Acta Derm Venereol 1994;74:201–5.
20. Zenzen V, Zankl H. *In vitro* evaluation of the cytotoxic and mutagenic potential of the 5-aminolevulinic acid hexylester-mediated photodynamic therapy. Mutat Res 2004;561:91–100.
21. van Renswoude J, Bridges KR, Harford JB, Klausner RD. Receptor-mediated endocytosis of transferrin and the uptake of fe in K562 cells: identification of a nonlysosomal acidic compartment. Proc Natl Acad Sci U S A 1982;79:6186–90.
22. Karagiannis TC, Lobachevsky PN, Martin RF. Cytotoxicity of an ^{125}I-labelled DNA ligand. Acta Oncol 2000; 39:681–5.
23. Kelly DP, Bateman, SA, Hook, RJ, et al. DNA binding compounds VI. Synthesis and characterization of 2,5′-disubstituted bibenzimidazoles related to the DNA minor groove binder, Hoechst 33258. Aust J Chem 1994;47:1751–69.
24. Gatter KC, Brown G, Trowbridge IS, Woolston RE, Mason DY. Transferrin receptors in human tissues: their distribution and possible clinical relevance. J Clin Pathol 1983;36:539–45.
25. Trowbridge IS. Transferrin receptor as a potential therapeutic target. Prog Allergy 1988;45:121–46.
26. Klausner RD, Van Renswoude J, Ashwell G, et al. Receptor-mediated endocytosis of transferrin in K562 cells. J Biol Chem 1983;258:4715–24.
27. Ciechanover A, Schwartz AL, Dautry-Varsat A, Lodish HF. Kinetics of internalization and recycling of transferrin and the transferrin receptor in a human hepatoma cell line. Effect of lysosomotropic agents. J Biol Chem 1983;258:9681–9.
28. Jin M, Snider MD. Role of microtubules in transferrin receptor transport from the cell surface to endosomes and the Golgi complex. J Biol Chem 1993; 268:18390–7.
29. Kim ES, Khuri FR, Herbst RS. Epidermal growth factor receptor biology (IMC-C225). Curr Opin Oncol 2001;13:506–13.
30. Ciardiello F, De Vita F. Epidermal growth factor receptor (EGFR) inhibitors in cancer therapy. Prog Drug Res 2005;63:93–114.
31. Sato JD, Kawamoto T, Le AD, Mendelsohn J, Polikoff J, Sato GH. Biological effects *in vitro* of monoclonal antibodies to human epidermal growth factor receptors. Mol Biol Med 1983;1:511–29.
32. Jones SM, Foreman SK, Shank BB, Kurten RC. EGF receptor downregulation depends on a trafficking motif in the distal tyrosine kinase domain. Am J Physiol Cell Physiol 2002;282:C420–33.
33. Beissert S, Schwarz T. Role of immunomodulation in diseases responsive to phototherapy. Methods 2002;28: 138–44.

Downloaded from cancerres.aacrjournals.org on April 13, 2017. © 2006 American Association for Cancer Research.

AACR American Association for Cancer Research

Cancer Research

The Journal of Cancer Research (1916–1930) | The American Journal of Cancer (1931–1940)

Receptor-Mediated DNA-Targeted Photoimmunotherapy

Tom C. Karagiannis, Pavel N. Lobachevsky, Brenda K.Y. Leung, et al.

Cancer Res 2006;66:10548-10552.

Updated version	Access the most recent version of this article at: http://cancerres.aacrjournals.org/content/66/21/10548
Supplementary Material	Access the most recent supplemental material at: http://cancerres.aacrjournals.org/content/suppl/2006/10/31/66.21.10548.DC1

Cited articles	This article cites 32 articles, 7 of which you can access for free at: http://cancerres.aacrjournals.org/content/66/21/10548.full.html#ref-list-1

E-mail alerts	Sign up to receive free email-alerts related to this article or journal.
Reprints and Subscriptions	To order reprints of this article or to subscribe to the journal, contact the AACR Publications Department at pubs@aacr.org.
Permissions	To request permission to re-use all or part of this article, contact the AACR Publications Department at permissions@aacr.org.

Downloaded from cancerres.aacrjournals.org on April 13, 2017. © 2006 American Association for Cancer Research.